Numerical Simulation of Canal Seepage During Construction Period Using Improved Node Virtual Flow Method

Pei CHUAN-KANG[1], Wei BING-QIAN[1], Yang PO[1]
1. College of Water Resources and Hydro-power Engineering, Xi'an University of Technology. Xi'an,710048, China
E-mail: eurastaer@outlook.com

Abstract: This study used the improved node virtual flow method to investigate the seepage field of a large-scale canal project during construction period, with different dewatering well configurations corresponding to the design cases P1 to P5. In this simulation, the water head distribution, pump discharge and seepage gradient in different cases were obtained and analyzed. By controlling the pumping level of the dewatering well, the relationship between the pumping level and the groundwater level was studied. The results show that reasonable precipitation arrangement can effectively reduce the groundwater level of the foundation pit and provide a strong guarantee for the safe operation of the project.
Keywords: improved node virtual flow method; finite element simulation; seepage field; dewatering well; canal model

1. Introduction

Canal seepage is one of the most important causes of water loss and structure instability, so it is thus beneficial understanding the process of canal seepage and seepage field distribution to ensure the safety and seepage stability of the canal project. For large canal project where the underground water level is high and the permeability coefficient of soil is small during the construction period, whether the groundwater level can be reduced has a great influence on the process of construction. Therefore, the seepage field and dewatering measures during the construction period should be studied in order to meet the needs of the safety and stability of the large-scale canal engineering.

During the construction period, the arrangement of the canal dewatering well has a great influence on the water head distribution of the seepage field. In traditional engineering, the equations for the design of canal dewatering measures in construction period depends on a number of idealized assumptions, and it is also very difficult to select the appropriate value for some important calculation parameters (such as dewatering well influencing radius). Although the traditional methods of simple application, but many restrictions. In recent years, with the development of computer technology and numerical methods related to unconfined seepage problem with free surface, researchers gradually began to use numerical simulation to solve the problem of canal seepage and made a series of contributions. Homayoon et al. [1] using the finite element method strictly simulated the lining effect on channel seepage field. Li BIN et al. [2] simulated the process of canal seepage under different engineering schemes using the improved cut-off negative pressure method. Asharf et al. [3] took a channel engineering as an example, compared the seepage simulation results in specific hydraulic structures under different dimensions. Zhong DENG-HUA et al. [4] used N-S equation coupled with VOF method to analyze the seepage stress of a channel section in the middle route of South to North Water Diversion project. Cui HAO-DONG et al. [5] developed the node virtual flow method and evaluated the effects of different kinds of seepage control measures. Wang JIN-LONG et al. [6] use MODFLOW in GMS to build three-dimensional canal model and calculated a number of factors that significantly affect the seepage field.

The above research showed the effectiveness and practicability of the numerical simulation in engineering application, and the predicted results may provide guidance for engineering practice. However, besides the aforementioned studies of canal seepage, there is little detailed work on the influence of different dewatering well arrangement on the seepage control effect, due to the limitation of the calculation method, the calculation efficiency is low under the condition of steady seepage conditions. Su BAO-YU et al. [7] proposed the node virtual flow method which identify the seepage free surface without change the meshes, based on that, Cui HAO-DONG et al. [8] put forward the improved node virtual flow method, and validated the method by engineering practice. The results showed the reliability and superiority of this method. Therefore, to investigate the effects of this characteristics and their relationships of a real canal project, the improved node virtual flow method was applied in the South-to-North water diversion project (Northeast China) to simulate the seepage field under construction period. This mathematical model strictly deducts the contribution of virtual flow in transition zone，thus the seepage field of free surface and seepage overflow point can be described more precisely, and the simulation results was proved to be more accurate than other methods used in canal or dike projects.

Based on the above efforts, the improved node virtual flow method was applied to solve the seepage field and the equivalent node flow method was applied to solve the exact solution of pumping discharge. These efforts aimed to identify and quantify different dewatering well arrangements influencing canal seepage so to provide reference for the construction of the canal project under similar conditions.

2. Mathematical model description

2.1. Unconfined seepage field calculating model

According to the continuity condition of water flow and the generalized Darcy's law, the governing equation of steady saturated seepage problem in anisotropic porous media is:

$$-\frac{\partial}{\partial x_i}\left(k_{ij}\frac{\partial h}{\partial x_j}\right)+Q=0 \qquad (1)$$

where x_i is the space coordinate, k_{ij} is the saturated permeability coefficient tensor describing permeability anisotropy of rock mass, h is the water head and Q is the source or sink term.

Fig. 1 depicts the calculating boundary of unconfined steady seepage field and the boundary conditions are as follows:

$$h\big|_{\Gamma_1}=h_1 \qquad (2)$$

$$-k_{ij}\frac{\partial h}{\partial x_j}n_i\big|_{\Gamma_2}=q_n \qquad (3)$$

$$-k_{ij}\frac{\partial h}{\partial x_j}n_i\big|_{\Gamma_3}=0, h=x_3 \qquad (4)$$

$$-k_{ij}\frac{\partial h}{\partial x_j}n_i\big|_{\Gamma_4}\geq 0, h=x_3 \qquad (5)$$

where h_1 is the known water head, n_i is the outer normal direction cosine of seepage boundary surface, $i=1,2,3$. Γ_1 is the known water head boundary, Γ_2 is the seepage boundary with known seepage discharge, Γ_3 is the seepage overflow surface, Γ_4 is the seepage free surface, and q_n is the boundary normal flow function, in here the outflow is positive.

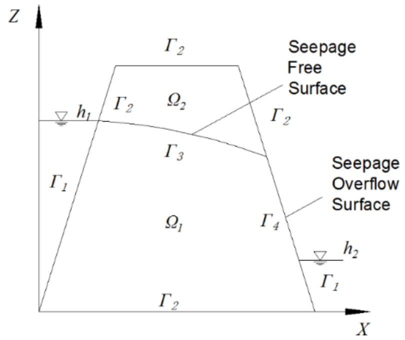

Fig. 1 Calculating boundary of unconfined seepage field

2.2 Improved node virtual flow method

For the seepage problem in the last section, taken unconfined seepage model (shown in Fig.1) as an example, seepage free surface divided the whole calculating domain into two parts, which were named as Ω_1 (seepage actual domain) and Ω_2 (seepage virtual domain). Since the position of the free surface and the outflow point are unknown, it is necessary to solve the problem by multi-step iteration. By solving this mathematical model, the Galerkin weighted residual method was applied, and the governing equation of the corresponding finite element solution was obtained:

$$[K]\{h\} = \{Q\} - \{Q_2\} + \{\Delta Q\}, \{\Delta Q\} = [K_2]\{h\} \quad (6)$$

where $[K]$, $\{h\}$ and $\{Q\}$ respectively denote the total conduction matrix, node water head array and node equivalent flow array in calculating domain Ω. $\{\Delta Q\}$ is the node virtual flow array contributed by the seepage virtual domain Ω_2. $[K_2]$ is the conduction matrix contributed by the seepage virtual domain Ω_2.

In the above parameters, the conduction matrix $[K_2]$ is the most difficult to solve properly for the part of the conduction matrix $[K_2]$ is contributed by the pure virtual elements, and the other part is contributed by the virtual zone of the transition elements. In order to improve the calculating accuracy of $[K_2]$, the encrypted Gauss point technique and the continuous penalty function were applied to solve the conduction matrix contributed by the virtual zone of the transition element, which is $[K]^e$:

$$[K]^e = \sum_{i}^{n_g}\sum_{j}^{n_g}\sum_{m}^{n_g} W_i W_j W_m \left(1 - H_\varepsilon(p)\right) F\left(\xi_i, \eta_j, \zeta_m\right) \quad (i, j, m = 1, 2, 3) \quad (7)$$

where i, j, m are the space coordinates, n_g is the encrypted number of Gauss point, W_i, W_j, W_m is the weight of each coordinate, $F\left(\xi_i, \eta_j, \zeta_m\right)$ is the integrand and inside the brackets are the Gauss point coordinates, $H_\varepsilon(p)$ is the continuous penalty function.

3. Dewatering design schemes of canal project

A section of the South-to-North Water Diversion Project, located in north Shandong province, was selected as a case study while under construction period. Its 11.989km long and the bottom width of the canal is 25m. The average elevation of the canal bottom is 28.1m, and the crest elevation of levee is 34.43m. This canal use dewatering wells to keep the construction site dry and convenient to construct. Canal works rich in groundwater, so in order to ensure the construction requirements and construction quality, the seepage field of the canal engineering should be calculated and analyzed. The soil information of canal's typical section is shown in Fig.3 and Fig.4.

The permeability coefficient is related to many factors. According to the preliminary survey data, the simplified permeability coefficient of each soil layer is shown in table 1. Assuming that canal's groundwater table is equal in the left and right bank, the foundation pit has been formed, without considering the drainage of the excavation process. Canal is not lining or set any drainage measures. In this simulation, the evaporation effect is ignored, the water in the soil is assumed incompressible, the soil is assumed to be homogeneous and its properties remains unchanged in the seepage simulation process. Based on the above assumptions, the simulation domain is generalized to be a homogeneous three-dimensional steady seepage system.

Table 1 Permeability coefficient of soil

Number	Lithology	Permeability Coefficient (K)	
		cm/s	m/d
1	Clay	2.6×10^{-3}	2.23
2	Loam	2.0×10^{-3}	1.73
3	Clay	5.9×10^{-4}	0.51
4	Loam	1.1×10^{-3}	0.93
5	Fine Sand	5.0×10^{-3}	4.32

For the convenience and efficient of seepage simulation, the circular well is simplified to 600mm*600mm square well in equal area. The calculation model takes a half of the area along the longitudinal direction of the canal which is influenced by a set of the dewatering wells. Both the upstream and downstream boundaries of the canal were considered as the impermeable boundary surface, the left and right bank of the canal are known as the deterministic water head boundary surface, the slope and the bottom of the canal are considered as the overflow boundary surface, and the boundary of the well is set up as the overflow boundary surface to control the water discharge. The eight-node hexahedron element is used to calculate, the number of nodes in the basic model is 48474, and the number of elements is 43292. Fig.2 depicts the FEM calculating meshes and dewatering well detail meshes, the meshes of other cases is slightly different.

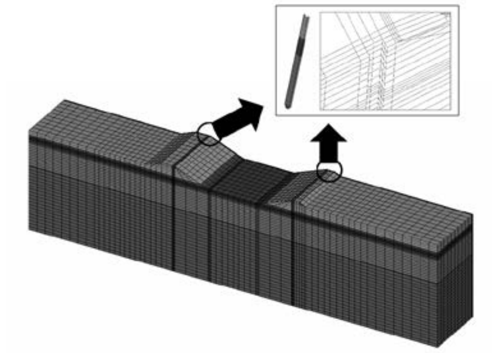

Fig. 2 3D FEM calculating meshes and dewatering well detail meshes

The Cartesian coordinate system is established based on the midpoint of the lowest excavated surface of the canal project. The X axis points the right to left bank direction of the canal, the Y axis points the direction along the canal longitudinal, and the Z axis is the height. The following involved value of the water table are all based on this coordinate system. The basic case (P1) in table 2 uses double dewatering wells in a set to control the seepage. The longitudinal spacing along the canal direction between two sets of dewatering wells is 60m, the embedded depth is 20m, and the non-fines concrete pipe is applied in the dewatering well. The typical cross section of canal in double wells arrangements is shown in Fig.3. In addition, case of P3 and P5 uses single dewatering well arranged in the longitudinal axis of the canal to control the seepage, and the embedded depth is 12m. The typical cross section of canal in single well arrangements is shown in Fig.4 and the detail of calculation cases is shown in Table 2.

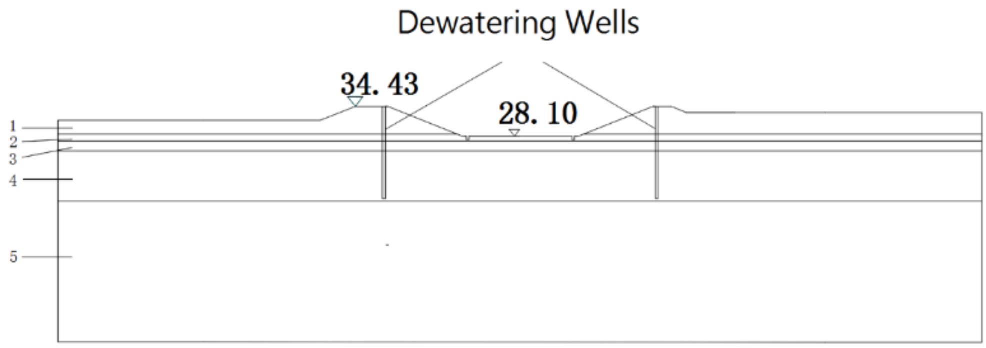

Fig. 3 Typical cross section of canal in double wells arrangement

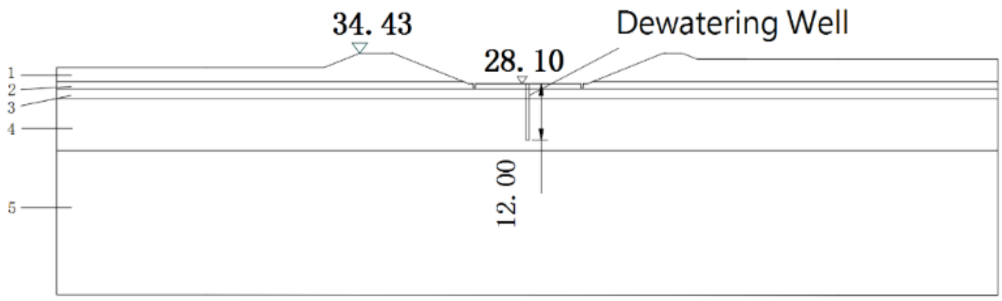

Fig. 4 Typical cross section of canal in single well arrangement

Table 2 The cases of calculation

Case	Flood Season	Groundwater Level/m	Longitudinal Well Spacing/m	Well Arrangement
P1	Non Flood Season	1.75	60	Double Wells
P2	Non Flood Season	1.75	25	Double Wells
P3	Non Flood Season	1.75	25	Single Well
P4	Flood Season	2.75	25	Double Wells
P5	Flood Season	2.75	25	Single Well

4. Simulation results and discussion

4.1 Distribution of water head contour in the well-midpoint cross section

Setting the water level of dewatering wells as -4m to calculate current seepage field, and the contours of water head distribution in the well-midpoint cross section were shown in Fig.5-9. Fig.5 depicts the water head contour of case P1, the contour lines are well distributed and reflects how boundary conditions and seepage control measures influenced seepage field. The free surface varies from groundwater table in the right and left bank of the canal (1.75m) to -4m around the dewatering wells, and decreases significantly near two wells, the water head contour lines are relatively more densely distributed. The water head contour lines are reasonable distributed in the seepage field, and the dewatering well works well, too. However, the free surface of seepage uplifted at the bottom of the canal and its water head is only -0.24m, which does not meet the requirement that the groundwater table should be decreased below 0.5m from the lowest excavation surface in the dry-land construction.

Fig.6 shows the water head contour of the P2 section, the free surface at the bottom of the canal is much lower than case P1, and the distribution of water head contour lines are much sparse than that of P1. These phenomena indicate that once the distance between two sets of dewatering wells in the longitudinal direction were shortened, the number of dewatering wells is relatively increased, thus benefits the effect of seepage control and depressurization. In case P2, the maximum height of seepage free surface at the bottom of the canal is -1.148m, which meets the requirement of dry-land construction, and has a good effect of seepage control.

Compared with P2, P3 changed the seepage control measures into single dewatering well arrangement, and the well is constructed in the center of the canal bottom. Fig.7 shows that even case P3 reduced the depth and the number of dewatering wells in a great amount, and the head water head contour lines near the well were distributed more densely, yet the engineering quantities are reduced, and the maximum seepage free surface water level at the bottom of the canal (-0.579m) meets the requirement of the dry-land construction, which is more economical and reasonable than the previous two cases.

As we can see from Fig.8 and Fig.9, case P4&P5 elevated the groundwater table to 2.75m than case P2&P3. The water head distribution is significantly denser than the previous three cases, and the free surface rises in the bottom of the canal. This indicates that the groundwater table has an obvious influence on seepage control effect. Therefore, the investigation of underground water level should be enhanced in the preparation of engineering project, the effect of seepage control measures in different groundwater tables also should be taken into account.

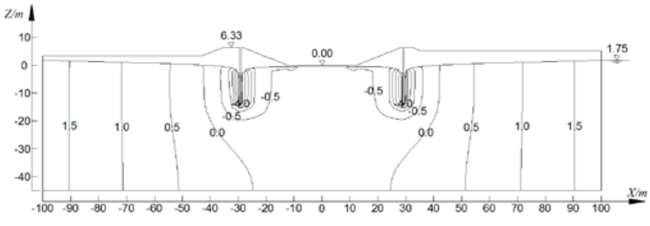

Fig. 5 Contour of water head of case P1

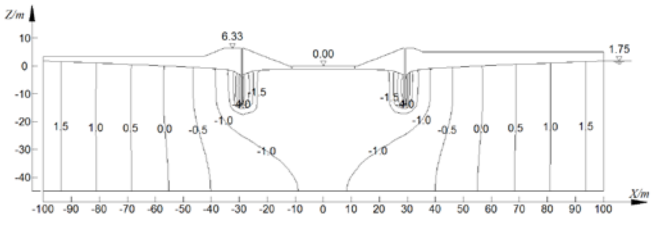

Fig. 6 Contour of water head of case P2

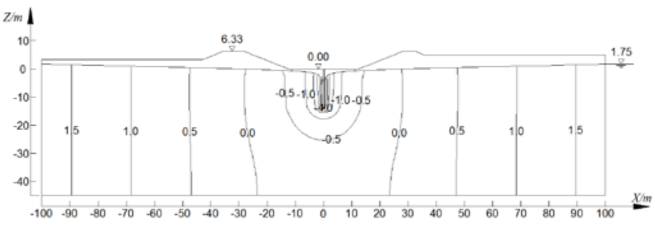

Fig. 7 Contour of water head of case P3

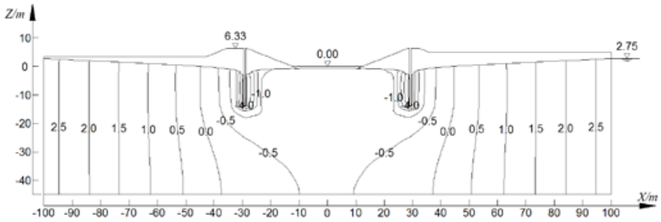

Fig. 8 Contour of water head of case P4

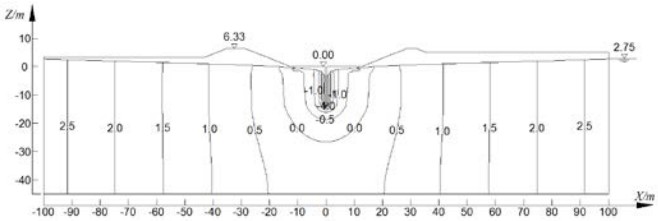

Fig. 9 Contour of water head of case P5

4.2 Analysis of hydraulic gradient in the boundary of dewatering wells

The negative gradient direction of the water head value is the seepage flow direction. From the above research, we can see that the water head contour lines distributed more densely near the dewatering wells which makes this area more easily destructed. Besides, the interface between the loam layer and fine sand layer is also worth paying extra attention due to the large difference in permeability coefficient between two layers. To further study this issue, the water level of dewatering wells was set as -4m to calculate the hydraulic gradient in the boundary of the well and the interface between the loam layer and fine sand layer. Fig.10 shows the maximum hydraulic gradient in each case. For the double wells arrangement cases, the boundary of the well in the left side which provides the maximum hydraulic gradient was selected to analyze.

According to Fig.10, for the boundary of the dewatering well, the hydraulic gradient in case P1 is greater than the other four cases, thus it could be more likely destructed compared to other cases. The value of P2&P3 is relatively small than P1, indicating that the denser the well arranges, the smaller possibility the seepage failure happens. Compared P2 to P4, P3 to P5, we can see that the value of the hydraulic gradient is very sensitive to the groundwater level in the same seepage control measures. The higher the initial groundwater level is, the more easily the seepage failure occurs. Among five cases, case P3 has the minimum gradient value, which makes it the most stable case of all.

For the interface between two soil layers, the value of five cases are very close and all very small compared to the values in the boundary of the dewatering well. This shows that the internal soil seepage gradient is relatively small in this condition.

The stability of canal structure is not only related to the hydraulic gradient, but also the gradation and particle size of soil mass. Besides, the interrelationship between layers also played an important role. In the construction period, long-time seepage control may lead to stratum settlement, hence the development and evolution mechanism of seepage destruction for the area with the risk must be further analyzed to provide a reliable guarantee for the engineering practice.

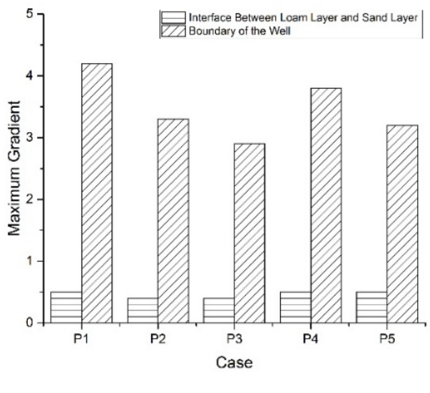

Fig.10 Comparison of maximum hydraulic gradient calculation results of cases

4.2 Analysis of hydraulic gradient in the boundary of dewatering wells

Change the pumping water level of the dewatering well and calculate the single-well pump discharge and seepage field, the results are shown in Fig.11 and Fig.12.

1) Effects of dewatering well arrangement on single-well pump discharge

The quantity of pumping has a great influence on the groundwater level at the bottom of the canal, and also reflects the dewatering capacity of the well. As shown in Fig.11, with the deepening of the pumping level of the well, the pump discharge gradually increases, and showed the trend of a gradual slowdown, indicating that the pumping capacity of the dewatering well is saturated by degrees.

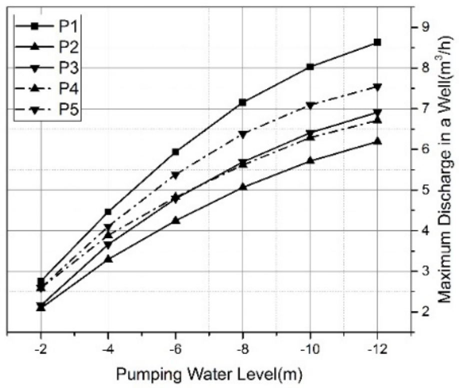

Fig. 11 Relationship between water level and maximum pump discharge in a dewatering well

Because of the large distance between two sets of dewatering wells along the canal direction in case P1, one set of wells could affect a wide area, thus the discharge in different pumping water level that case P1 produced is the greatest among all other cases. Compared with P1, the overall pump discharge of P2 decreased in an obvious way, demonstrating that the variation of the Y direction of two sets of wells has a significant effect on the pump discharge. Case P3 applied single-well arrangement, hence the discharge is greater than P2. Contrast P2 to P4 and P3 to P5, we can find out that in the same seepage control scheme, the increase of the initial groundwater level leads to greater pump discharge, which has a great influence on the seepage control results. thus, attention should be paid to this connection.

2) Effects of dewatering well arrangement on water level down the canal bottom

Fig.12 shows the relationship between pumping water level and minimum buried depth of the groundwater. The horizontal auxiliary line at ordinate 0.5m stand limits for dry-land construction. As shown in the figure, with the deepening of well's pumping level, the groundwater level continues to decrease, and the buried depth of the groundwater increases. The groundwater level at the bottom of the canal in case P1 and P5 is the closest to the canal's lowest excavated surface. In the horizontal coordinate -2m and -4m, the minimum buried depth of the groundwater is all less than 0.5m, which does not meet the requirement of dry-land construction. When the pumping level reaches -6m or deeper, the groundwater buried depth of all cases is greater than 0.5m, meets the requirement of dry-land construction. Therefore, it is considered that this project will be more economical and reasonable selecting the pumping level of the well at -6m.

Compared P2 to P4 and P3 to P5, under the same seepage control scheme, the minimum buried depth increases with the rises of initial given groundwater level. Besides, the decrease of pump discharge of wells will also lead to the rise of groundwater level at the bottom of the canal. The over-high groundwater level at the bottom of the canal is unfavorable to the construction of the canal, so it is necessary to strictly control the pumping depth of the well.

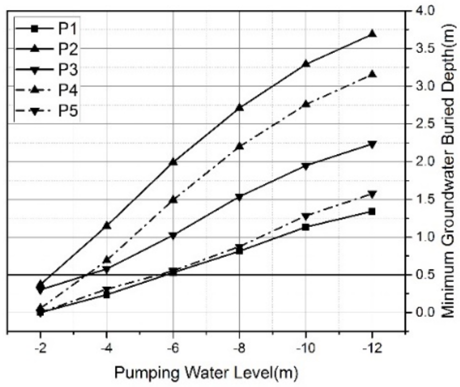

Fig. 12 Relationship between water level in a dewatering well and minimum buried depth of groundwater level in canal bottom

When the pumping level of dewatering well is relatively low, although the discharge is small, the groundwater level at the bottom of the canal is too high, but once the pumping level is too deep, it will affect the geological environment around the project, resulting in land subsidence and waste of groundwater resources. Accordingly, it is necessary to properly choose the pumping level of the dewatering well, and arrange the well position symmetrically and evenly, to make the engineering practice safely and reasonable.

5. Conclusions

In this paper, the node virtual flow method was used in a section of the South-to-North water diversion project (Northeast China) to simulate the seepage field under different seepage control schemes and boundary conditions in construction period. The results showed that single well arrangement can effectively reduce groundwater level on the premise of meeting the requirement of canal pit dewater, furthermore, this arrangement also reduced the quantities of the construction and the possibility of seepage failure, so it is the most reasonable and cost-effective arrangement.

The vertical spacing along the canal direction between two sets of dewatering wells should be selected reasonably since it affects the seepage control results in a big way. The smaller the vertical spacing of wells, the smaller the pump discharge and the better the dewatering results. It is also very important to select the proper pumping level of the dewatering well for the construction period, deeper pumping level could significantly increase the single-well discharge and lower the groundwater table at the bottom of the canal, accordingly, it is necessary to properly choose the pumping level of the dewatering well, and arrange the well position symmetrically and evenly. In this canal project, the case can be both cost-effective and reasonable when the pumping depth is at -6m.

The denser the dewatering well arranges, the smaller possibility the seepage destruction happens around the well. Besides, the value of the hydraulic gradient is very sensitive to the groundwater level in the same seepage control measures. The higher the initial groundwater level is, the more easily the seepage failure occurs. Therefore, the investigation of groundwater level should be strengthened in the preparatory period of the project.

References

[1] Homayoon Katibeh. Seepage from lined canal using finite-element method. Journal of Irrigation and Drainage Engineering, ASCE, 2004, 130(5): 441-444.

[2] LI Bin, LING Xiao, SONG Zhiyu. Analysis of seepage simulation of underground water sealed caverns in Jinzhou. Journal of Yangtze River Scientific Research, 2009, 26(10): 82-91. (in Chinese)

[3] Ashraf A.Ahmed, Abdallsh S. Bazaraa. Three-Dimensional analysis of seepage below and around hydraulic structures. Journal of Hydraulic Engineering, ASCE, 2009, 14(3): 243-247.

[4] ZHONG Denghua, ZHANG Xiaoxin, AO Xuefei, et al. Study on coupled 3D seepage and stress fields of the complex channel project. Sci China Tech Sci, 2013, 43(11): 1993-1201.

[5] CUI Haodong, ZHANG Jiafa, ZHANG Wei, al et. Numerical analysis of seepage field for typical canal stretch on confined aquifer of middle route project of south-to-north water transfer. Rock and Soil Mechanics, 2010, 31(S2): 447-452. (in Chinese)

[6] WANG Jinlong, ZHANG Jiafa, CUI Haodong, al et. Dewatering measures for construction period of the typical canal stretch of middle route project of SNWT. Journal of Zhengzhou University (Engineering Science), 2012, 33(5): 82-86. (in Chinese)
[7] SU Baoyu, ZHU Yueming. Procedure of virtual flux for eepage free surface with fixed mesh. Journal of Hohai University, 1991, 19(5): 113－117. (in Chinese)
[8] CUI Haodong, ZHU Yueming. Improved procedure of nodal virtual flux of global iteration to solve seepage free surface. Journal of Wuhan University of Technology, 2009, 33(2): 238-241. (in Chinese)
[9] ZHU Yueming. Darcy seepage discharge calculation with node method. Journal of Hohai University, 1991, 25(4): 105-108. (in Chinese)
[10] WANG Xinmin. Numerical analysis of engineering structure with ANSYS. Beijing: People's Communication Press. 2007. (in Chinese)
[11] QI Shuwen. Research on calculation method of seepage discharge for complicated 3D seepage flow field based on FEM. Nanjing: Hohai University, 2007. (in Chinese)
[12] MAO Changxi. Seepage computation analysis and control. Beijing: China Water Power Press. 2003. (in Chinese)
[13] ZHONG Denghua, ZHANG Xiaoxin, AO Xuefei, et al. Study on coupled 3D seepage and stress fields of the complex channel project. Sci China Tech Sci, 2013, 43(11): 1993-1201.
[14] A.K. Rastogi, Baldev Prasad. FEM modelling to investigate seepage losses from the lined Nadiad canal, India. Journal of Hydrology, 1992, 138: 153-168.
[15] ZHANG Wei, LI Sishen. Cloggingt mechanism and treatment measures for relief wells in dyke engineering. Journal of Yangtze River Scientific Reasearch Institute, 2006, 23(5): 24-28. (in Chinese)
[16] Bruch Jr., John C. Seepage streams out of canals and ditches overlying shallow water tables. Journal of Hydrology, 1979, 41(1): 31-41.
[17] Kang, T. Comparison of seepage analysis methods based on finite elements. Computer Methods and Recent Advances in Geomechanics-Proceedings of the 14th int. Conference of International Association for Computer Methods and Recent Advances in Geomechanics, IACMAG 2014, 2015: 1421-1426.
[18] Goyal, R. Chawla, A.S. Seepage from canals with infiltration from free zone surface. Journal of Irrigation and Drainage Engineering, 1997, 123(4): 257-263.
[19] WANG Hui, GAO Yating, QIN Qinghua. Green's function based finite element formulations for isotropic seepage analysis with free surface. Latin American Journal of Solids and Structures, 1979, 12(10): 1991-2005.
[20] LI Mingchuan, YAO Jun, GE Jiali. Research progress and development on seepage mechanics. Chinese Quarterly of Mechanics, 2012, 33(1): 74-80. (in Chinese)
[21] HE Wubin, CUI Xiangdong, LIU Yanzhong. Simulation research on surrounding environment influenced by pit excavation and dewatering well spacing. Journal of Taiyuan University of Technology, 2013, 44(3): 381-384. (in Chinese)
[22] SUN Ronglin, LIANG Xing, ZHANG Xiaolun, et al. Application of numerical modeling to dewatering design for foundation pit. Chinese Journal of Rock Mechanics and Engeering, 2003, 22(1): 2333-2337. (in Chinese)